

Orbital fluctuations in the different phases of LaVO_3 and YVO_3

M. De Raychaudhury,^{1,2} E. Pavarini,^{3,4} and O.K. Andersen¹

¹Max-Planck-Institut für Festkörperforschung, Heisenbergstrasse 1, D-70569 Stuttgart, Germany

²S.N. Bose National Centre for Basic Sciences, Kolkata 700098, India

³Institut für Festkörperforschung, Forschungszentrum Jlich, D-52425 Juelich, Germany

⁴CNISM-Dipartimento di Fisica "A. Volta", Università di Pavia, Via Bassi 6, I-27100 Pavia, Italy

We investigate the importance of quantum orbital fluctuations in the orthorhombic and monoclinic phases of the Mott insulators LaVO_3 and YVO_3 . First, we construct *ab-initio* material-specific t_{2g} Hubbard models. Then, by using dynamical mean-field theory, we calculate the spectral matrix as a function of temperature. Our Hubbard bands and Mott gaps are in very good agreement with spectroscopy. We show that in orthorhombic LaVO_3 , quantum orbital fluctuations are strong and that they are suppressed *only* in the monoclinic 140 K phase. In YVO_3 the suppression happens already at 300 K. We show that Jahn-Teller *and* GdFeO_3 -type distortions are both crucial in determining the type of orbital and magnetic order in the low temperature phases.

PACS numbers: 71.27.+a, 71.30.+h, 71.15.Ap

The Mott insulating t_{2g}^2 perovskites LaVO_3 and YVO_3 exhibit an unusual series of structural and magnetic phase transitions (Fig. 1) with temperature-induced magnetization reversal phenomena [1] and other exotic properties [2, 3]. While it is now recognized that the V- t_{2g} orbital degrees of freedom and the strong Coulomb repulsion are the key ingredients, it is still controversial whether classical (orbital order) [1, 4, 5, 6, 7, 8] or quantum (orbital fluctuations) [2, 9] effects are responsible for the rich physics of these vanadates.

At 300 K, LaVO_3 and YVO_3 are orthorhombic paramagnetic Mott insulators. Their structure (Fig. 2) can be derived from the cubic perovskite ABO_3 , with $\text{A}=\text{La}, \text{Y}$ and $\text{B}=\text{V}$, by tilting the VO_6 octahedra in alternating directions around the \mathbf{b} -axis and rotating them around the \mathbf{c} -axis. This GdFeO_3 -type distortion is driven by AO covalency which pulls a given O atom closer to one of its four nearest A-neighbors [10, 11]. Since the Y $4d$ level is closer to the O $2p$ level than the La $5d$ level, the AO covalency increases when going from LaVO_3 to YVO_3 and, hence, the shortest AO distance decreases from being 14 to being 20 % shorter than the average, while the angle of tilt increases from 12 to 18° , and that of rotation from 7 to 13° [12, 13]. Finally, the A-cube is deformed such that one or two of the ABA body-diagonals is smaller than the average by, respectively, 4 and 10 % in LaVO_3 and YVO_3 . These 300 K structures are determined mainly by the strong covalent interactions between O $2p$ and the empty B e_g and A d orbitals, hardly by the weak interactions involving B t_{2g} orbitals, and are thus very similar to the structures of the t_{2g}^1 La and Y titanates [10, 11].

The t_{2g}^2 vanadates, however, have a much richer phase diagram than the t_{2g}^1 titanates. At, respectively, 140 K and 200 K, LaVO_3 and YVO_3 transform to a monoclinic structure in which \mathbf{c} is turned slightly around \mathbf{a} whereby the two subcells along \mathbf{c} , related by a horizontal mirror plane in the orthorhombic structure, become independent (Fig. 2). Most important: a sizable (3-4%) Jahn-Teller

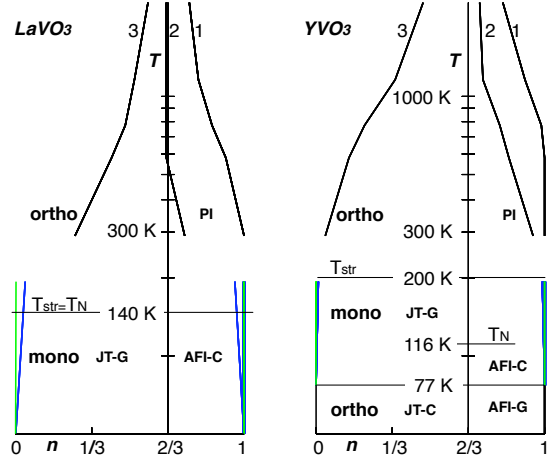


FIG. 1: Temperature-dependent structural and magnetic phases of LaVO_3 and YVO_3 . The lines show LDA+DMFT (quantum Monte Carlo [21]) results for the occupations, n , of the three t_{2g} crystal-field orbitals, 1, 2, and 3 (Table I). Black lines: orthorhombic phases. Green and blue lines: monoclinic, sites 1 and 3 (see Fig. 2). For each structure we calculated the occupations down to the temperature at which the orbital polarizations are essentially complete ($T \sim 200$ K) and then extrapolated in a standard way [21] to $T=0$ K.

(JT) elongation of a VO bond, that along \mathbf{y} in cells 1 and 4, and along \mathbf{x} in cells 3 and 2, deforms the VO_6 octahedra. At about 140 in LaVO_3 and 116 K in YVO_3 , antiferromagnetic C-type order develops (FM stacking of AFM *ab*-layers). At 77 K, YVO_3 recovers the orthorhombic structure and the magnetic order changes from C- to G-type (3D-AFM), while the long VO bond becomes that along \mathbf{x} in cells 1 and 3, and along \mathbf{y} in 2 and 4.

It has been suggested [1] that these phase transitions are driven by the changes in a static orbital order (OO) following the observed pattern of JT-distortions [4, 14]. According to this JT-OO model, which assumes that the

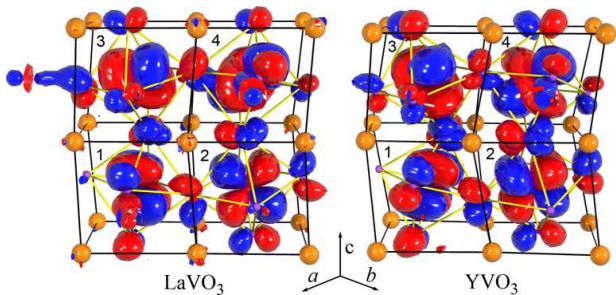


FIG. 2: Primitive cell containing four ABO_3 units. A-ions are orange, B-ions are at the centers of yellow O-octahedra. In terms of the primitive translation vectors, \mathbf{a} , \mathbf{b} , and \mathbf{c} the global \mathbf{x} , \mathbf{y} , and \mathbf{z} axes, directed approximately along the BO bonds, are: $\mathbf{x} = \mathbf{a}/(2+2\alpha) + \mathbf{b}/(2+2\beta)$, $\mathbf{y} = -\mathbf{a}/(2+2\alpha) + \mathbf{b}/(2+2\beta)$ and $\mathbf{z} = (\mathbf{c} - \mathbf{c} \cdot \mathbf{b})/(2+2\gamma)$. Here, α , β , and γ are small and $|\mathbf{x}| = |\mathbf{y}| = |\mathbf{z}| = 3.92\text{\AA}$ (3.82\AA) for LaVO_3 (YVO_3). The B-containing bc -plane glide-mirrors (with translation $(\mathbf{b} - \mathbf{a})/2$) unit 1 in 2 and 3 in 4, and exchanges the local, B-centered x and y coordinates. In the orthorhombic Pbnm structure (but not in the monoclinic $P2_1/a$ structure), the A-containing ab -plane mirrors unit 1 in 3 and 2 in 4. The empty crystal-field orbitals $|3\rangle_i$ of the monoclinic phase were put on sites $i=1, 2, 3, 4$. Red (blue) indicate positive (negative) lobes.

crystal-field (CF) is due to the oxygen octahedra, the t_{2g} orbital which is *most* antibonding with the O $2p$ orbitals, i.e. $|sz\rangle$ where s is the direction of the *short* in-plane VO bond, is *empty*; the other two t_{2g} orbitals, due to Hund's rule coupling, are *singly* occupied. This OO is C-type in the orthorhombic structure and G-type in the monoclinic structure. Later, this JT-OO model was challenged by a theory which assumes that the two highest orbitals, $|xz\rangle$ and $|yz\rangle$, are basically degenerate so that orbital *fluctuations* play a key role [2, 9]. Recently, ab initio LDA+ U [6] calculations gave support to the JT-OO model.

In this Letter we show that in LaVO_3 quantum effects are strong down to 300 K, however they become negligible in the AF-C monoclinic phase. For YVO_3 orbital fluctuations are suppressed already at 300 K, and the 77 K magnetic transition is associated with a change of OO. We show that the CF splittings result not only from the JT-, but also from the GdFeO_3 -type distortions, and thus OO is intermediate between C- and G-type. The influence of the JT- and the GdFeO_3 -type distortion is, respectively, stronger and weaker than in the t_{2g}^1 titanates [10, 11, 15].

The electronic structure is calculated with the LDA+DMFT method [16], fully accounting for the orbital degrees of freedom [11]. First, we compute the LDA bands with the N^{th} -order muffin-tin-orbital (NMTO) method [17]; we obtain (for all structures) $\frac{1}{3}$ -filled t_{2g} bands separated by a ~ 0.5 eV gap from the empty e_g bands and by a ~ 2 eV gap from the filled O $2p$ bands. Next, we Löwdin downfold to $V t_{2g}$ and remove the energy dependence of the downfolded orbitals by “ N -ization” [17]. These orbitals are strongly localized, hav-

$ j\rangle_i$	ϵ_j	$ xy\rangle$	$ xz\rangle$	$ yz\rangle$	n_j	ϵ_j	$ xy\rangle$	$ xz\rangle$	$ yz\rangle$	n_j
ortho Pbnm LaVO_3 (300 K)						Pbnm YVO_3 (300 K)				
$ 1\rangle_1$	419	.44	.24	.86	.78	303	.56	-.21	.80	.96
$ 2\rangle_1$	472	.34	.84	-.42	.63	383	.83	.17	-.54	.53
$ 3\rangle_1$	511	-.83	.48	.29	.59	510	-.02	.96	.27	.51
mono $P2_1/a$ LaVO_3 (10 K)						$P2_1/a$ YVO_3 (100 K)				
$ 1\rangle_1$	393	.46	.11	.88	.82	285	.78	-.30	.55	.97
$ 2\rangle_1$	471	.86	.16	-.48	.63	360	.49	-.25	-.83	.58
$ 3\rangle_1$	539	-.19	.98	-.03	.55	525	.39	.92	-.05	.55
$ 1\rangle_3$	441	.71	-.46	-.53	.76	345	.77	.20	-.60	.88
$ 2\rangle_3$	453	.08	.77	-.64	.66	405	.62	-.44	.65	.56
$ 3\rangle_3$	531	-.70	-.41	-.58	.57	547	-.13	-.88	-.46	.45
ortho						Pbnm YVO_3 (65 K)				
$ 1\rangle_1$						313	.64	-.26	.72	.98
$ 2\rangle_1$						394	.72	.53	-.45	.60
$ 3\rangle_1$						517	-.27	.81	.53	.42

TABLE I: LDA crystal-field (CF) levels wrt the t_{1g} Fermi level, ϵ_j/meV ($j=1, 2, 3$), LDA CF orbitals at site i , $|j\rangle_i$, in terms of the cubic orbitals, $|xy\rangle$, $|xz\rangle$, and $|yz\rangle$ in the global \mathbf{x} , \mathbf{y} , \mathbf{z} axes defined in Fig. 2. n_j are LDA occupations. Orbitals at equivalent sites (see Fig. 2): $|j\rangle_2$ ($|j\rangle_4$) is $|j\rangle_1$ ($|j\rangle_3$) with $x \leftrightarrow y$; for the Pbnm structures $|j\rangle_3$ is $|j\rangle_1$ with $z \rightarrow -z$.

ing $V t_{2g}$ character only in their heads. Symmetric orthonormalization finally yields localized [18] t_{2g} Wannier functions and their corresponding Hamiltonian, H^{LDA} . The many-body Hamiltonian is then a material-specific t_{2g} Hubbard model, $\hat{H} = \hat{H}^{\text{LDA}} + \hat{U}$, where for the on-site Coulomb repulsion, \hat{U} , we use the conventional expression [19], $\hat{U} = \frac{1}{2} \sum_{im\sigma, m'\sigma'} U_{m\sigma, m'\sigma'} n_{im\sigma} n_{im'\sigma'}$, where $n_{im\sigma} = c_{im\sigma}^\dagger c_{im\sigma}$, and $c_{im\sigma}^\dagger$ creates an electron with spin σ in a t_{2g} Wannier orbital m at site i . The screened on-site Coulomb interaction is $U_{m\sigma, m'\sigma'} = U \delta_{m, m'} \delta_{\sigma, -\sigma'} + (U' - J \delta_{\sigma, \sigma'}) (1 - \delta_{m, m'})$, where J is the exchange term and $U' = U - 2J$ the average Coulomb repulsion. We solve \hat{H} in dynamical mean-field theory (DMFT) [20], using a quantum Monte Carlo [21] impurity solver and working with the full self-energy matrix, $\Sigma_{mm'}(\omega)$ [11]. Note that inversion is the only point symmetry of the V sites. The spectral matrix on the real ω -axis is obtained by analytic continuation [22]. We use $U=5$ eV and $J=0.68$ eV, values close to theoretical [14] and experimental [23] estimates, which also give the correct mass renormalizations/Mott gaps for orthorhombic t_{2g}^1 V/Ti oxides using the same computational scheme [10, 11].

Let us start by describing the LDA t_{2g} bands in the orthorhombic 300 K phase. Remarkably, the CF orbitals $|j\rangle_i$ (Table I, $j=1, 2, 3$), obtained by diagonalizing the on-site i block of H^{LDA} , the hopping integrals $t_{j,j'}^{i,i'}$ (Table II), the t_{2g} band-shapes and band-width W (Fig. 3) are rather similar to those of the t_{2g}^1 titanates. These similarities [24] are due to the similarity of the crystal

structures. Like in the titanates, the CFs are essentially determined by the GdFeO₃-type distortion, mainly via the A-ligand field, specifically the AB and AOB covalency. However, in the vanadates the CF splittings are about half those of the respective titanates and the CF orbitals [25] and the hopping integrals are less deformed by cation covalency [24]. This is due to the Ti → V substitution [26]: since V is on the right of Ti in the periodic table, the V 3*d* level is closer to the O 2*p* and further from the A *d* level than the Ti 3*d*. Thus the sensitivity of the B *t*_{2*g*} Wannier functions to GdFeO₃-type distortions decreases, while the sensitivity to JT increases.

Now, turning on the Coulomb repulsion transforms the metallic LDA density of states (DOS) into the spectral matrix of a Mott insulator (Fig. 3). For LaVO₃, the Mott gap is ~ 1 eV, in accord with optical conductivity data [27], and the Hubbard bands are centered around -1.5 eV and 2.5 eV, in very good agreement with photoemission and inverse photoemission [28]. For YVO₃, the gap is slightly larger, ~ 1.2 eV, in accord with optical data [27], and the Hubbard bands are centered around -1.5 eV and 3 eV, in agreement with photoemission [28].

The Mott gaps in the vanadates are somewhat *larger* than in the titanates, for which the measured gaps are ~ 0.2 eV in LaTiO₃ and ~ 1 eV in YTiO₃ [27], in line with LDA+DMFT results [11]. This could appear surprising: orbital degeneracy increases the critical ratio for the Mott transition, U_c/W , by enhancing the effective band-width, and the enhancement is stronger the closer the system is to half-filling [29]. So the gap should be smaller for a *t*_{2*g*} than for a *t*_{2*g*} system, everything else remaining the same. However, the Hund's rule exchange energy, J , strongly suppresses this enhancement, as shown for half-filling in Ref. 30. For $n=\frac{1}{6}$ and $n=\frac{1}{3}$, and using a 3-fold degenerate Hubbard model with a rectangular DOS, $T=770$ K, and $J/W \sim \frac{1}{3}$ (like in the vanadates where $J/W=0.68/1.9$), we find that the metal to insulator transition occurs for $U'/W \sim 1.5$ when $n=\frac{1}{6}$, and for $U'/W \sim 1.3$ when $n=\frac{1}{3}$. So the Hund's-rule coupling dominates, and thus the vanadates can have larger gaps than the titanates.

Like for the titanates [11], diagonalization of the DMFT occupation matrix yields three eigenvectors nearly identical to the LDA CF orbitals. For LaVO₃ at 770 K, the Coulomb repulsion only slightly increases the orbital polarization by changing the occupations as follows: 0.78→0.87, 0.63→0.65, and 0.59→0.48. Thus, surprisingly, orbital fluctuations are sizable and remain so down to room temperature: $n_3=0.26$ at 290 K. Due to the stronger cation covalency in YVO₃, the Coulomb repulsion causes substantial orbital polarization already at 770 K (see Fig. 1). At 300 K, we find that only $c_{2\sigma}^\dagger c_{1\sigma}^\dagger |0\rangle$, paramagnetic with $S=1$, is occupied. Thus, YVO₃ is orbitally ordered well above the magnetic phase transition; since, at site 1, $|3\rangle_1 \approx |xz\rangle$ (see Table I) is empty and thus $|xy\rangle$ and $|yz\rangle$ are \approx singly occupied, the OO happens to agree with the prediction of the JT-OO model [4, 6, 14]

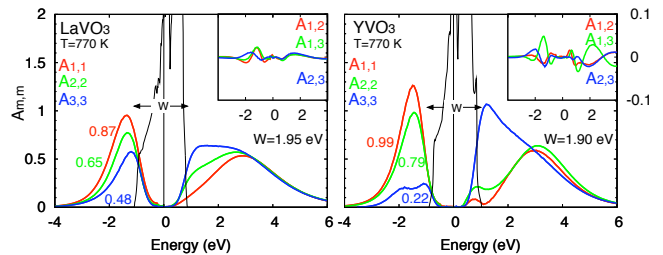


FIG. 3: (color on-line) LDA+DMFT spectral matrix $A_{m,m'}$ in the crystal-field basis. The off-diagonal terms are ~ 5 times smaller than in LDA. In black, the LDA DOS.

($|3\rangle_1 \approx -|3\rangle_3 \approx |xz\rangle$, $|3\rangle_2 \approx -|3\rangle_4 \approx |yz\rangle$), even though the CF is caused mainly by the GdFeO₃-type distortion.

What happens in the JT-distorted low temperature phases? The rms values of the hopping integrals hardly change, so W remains ~ 1.9 eV, but individual hopping integrals do change, even in the $|xy\rangle, |xz\rangle, |yz\rangle$ representation. Most affected are the CF orbitals (see Table I).

For LaVO₃, the CF splittings increase; this, in addition to the low temperature, lets the Coulomb repulsion suppress quantum effects entirely. At sites 1 and 2, the occupied state is in accord with the JT distortion (at site 1 $|xy\rangle$ and $|yz\rangle$ are singly occupied and $|3\rangle_1 \approx |xz\rangle$ is empty; at site 2, by symmetry, the empty state is $|3\rangle_2 \approx |yz\rangle$; see Fig. 2 and Tab. I) but this is not the case at sites 3 and 4 ($|3\rangle_3 \neq -|yz\rangle$, $|3\rangle_4 \neq |xz\rangle$). A static mean-field calculation (pseudopotential-based LDA+ U) [6] yields empty states not far from ours [31], but, without analyzing the results, the OO was ascribed to the JT distortions. In contrast, we find that the CF orbitals depend crucially also on the GdFeO₃-type distortions and that the OO is not of G-type, but is intermediate between C- and G-type.

For YVO₃, the CF splittings are similar to those of the 300 K phase, but quantum effects are negligible (Fig. 1). On *all* sites in the monoclinic structure the *empty* orbital is almost the same as in the orthorhombic 300 K phase so OO does *not* follow the JT distortions ($|3\rangle_1 \approx -|3\rangle_3 \approx |xz\rangle$, $|3\rangle_2 \approx -|3\rangle_4 \approx |yz\rangle$), but is almost C-type. In the orthorhombic 77 K phase, the empty orbital at site 1, $|3\rangle_1$, only roughly equals $|xz\rangle$. Our results are consistent with resonant x-ray scattering [5] and magnetization [1] data. LDA+ U [6] yields results close to ours [31].

Finally, we find that the monoclinic structure favors C-type magnetic order over G-type by increasing some hopping integrals $t_{j,j'}^{i,i'}$ (Table II) to the empty orbital $|3\rangle$ along the *c*-direction. Assuming complete OO, conventional theory yields, for the superexchange couplings,

$$J_{SE}^{i,i'} \sim \frac{1+J/U}{U+2J} \sum_{j,j' \leq 2} |t_{j,j'}^{i,i'}|^2 - \frac{J/U}{U-3J} \sum_{j \leq 2} (|t_{j3}^{i,i'}|^2 + |t_{3j}^{i,i'}|^2)$$

with j, j' CF orbitals and i, i' neighboring sites. We find that C-type order ($J_{SE}^{i,i+z} < 0$, $J_{SE}^{i,i+x} = J_{SE}^{i,i+y} > 0$) is fa-

$j, j' \setminus lmn$	La Pbnm			La P _{21/a} , site 1			La P _{21/a} , site 3			Y Pbnm			Y P _{21/a} , site 1			Y P _{21/a} , site 3			Y Pbnm (65 K)		
	001	100	010	001	100	010	001	100	010	001	100	010	001	100	010	001	100	010	001	100	010
1, 1	130	-65	-65	85	-39	-39	85	-159	-159	-13	-17	-17	-49	-84	-84	-49	-92	-92	-35	-34	-34
1, 2	9	-37	-198	27	-110	-127	-36	-65	98	-63	-102	-157	-20	-117	-62	-46	-73	-169	-38	-66	-195
1, 3	119	104	-7	154	31	-155	153	90	23	46	66	-138	30	11	-170	26	80	-91	52	100	-68
2, 2	193	47	47	-133	-84	-84	-133	94	94	86	-48	-48	72	-6	-6	72	25	25	142	-28	-28
2, 3	26	13	9	-57	76	73	-140	110	30	38	5	20	-112	9	94	118	-41	30	67	-27	7
3, 3	36	-152	-152	65	-38	-38	65	-109	-109	202	-66	-66	183	-48	-48	183	-63	-63	173	-61	-61

TABLE II: Hopping integrals $t_{j,j'}^{i,i'}$ /meV from site i to a site $i' = i + l\mathbf{x} + m\mathbf{y} + n\mathbf{z}$, in the basis (j, j') of crystal-field orbitals. Here $i=1$ and (P_{21/a} only) $i=3$. Notice that $t_{j,j'}^{i,i+z} = t_{j',j}^{i+z,i}$ and $t_{j,j'}^{i,i+x} = t_{j',j}^{i,i+y}$. For Pbnm structures only: $t_{j,j'}^{i,i+z} = t_{j',j}^{i,i+z}$.

vored over G-type, for which all couplings are positive, if $J/U \gtrsim 0.16$. While the actual values of $J_{SE}^{i,i'}$ are sensitive to details [6, 7, 10], this provides a microscopic explanation of C-type order in monoclinic LaVO₃ and YVO₃, the change from C- to G-type across the structural phase transition in YVO₃, and thus could also explain the magnetization-reversal phenomena [1].

In conclusion, we find that the orthorhombic LaVO₃ is one of the few Mott insulators which exhibits large quantum effects at room temperature. This is not the case for YVO₃ (and t_{2g}^1 titanates [11]). In the low temperature phases, orbital fluctuations are negligible for both vanadates. This supports the view [1, 4, 14] that the magnetic structures of the vanadates can be explained by orbital-order. Recent LDA+ U [6] and LDA+PIRG [8] calculations agree with this, but previous literature ascribed OO mainly to JT-distortions. In contrast, we proved that both the JT *and* the GdFeO₃-type distortions are crucial for the CF orbitals and their hopping integrals, and thus for the type of orbital and magnetic order. The effects of the GdFeO-type distortions are weaker and those of JT stronger than in t_{2g}^1 titanates; their interplay is responsible for the rich phase diagram of the vanadates.

We thank E. Koch, A.I. Lichtenstein, S. Biermann, and A. Georges for discussions and J. Nuss for graphics support. Computations were done on the Jülich BlueGene. M. D. thanks the MPG Partnergroup program.

we find (in meV) for P_{21/a} YVO₃ (LaVO₃): $J_{SE}^{i,i+z} = -1.8$ (-4.1), $J_{SE}^{1,1+x} = 0.06$ (3.0) and $J_{SE}^{3,3+x} = 7.1$ (7.6).

- [7] I. V. Solovyev, Phys. Rev. B **74**, 054412 (2006).
 [8] Y. Otsuka and M. Imada, cond-mat/0610012.
 [9] G. Khaliullin, P. Horsch and A. M. Oles, Phys. Rev. Lett. **86**, 3879 (2001); G. Khaliullin, Prog. Theor. Phys. Suppl. **160**, 155 (2005).
 [10] E. Pavarini, A. Yamasaki, J. Nuss and O. K. Andersen, New J. Phys. **7** 188 (2005).
 [11] E. Pavarini *et al.*, Phys. Rev. Lett. **92**, 176403 (2004).
 [12] P. Bordet *et al.*, J. Solid State Chem. **106**, 253 (1993).
 [13] G. R. Blake *et al.*, Phys. Rev. B **65**, 174112 (2002).
 [14] T. Mizokawa and A. Fujimori, Phys. Rev. B **54**, 5368 (1996).
 [15] M. Mochizuki and M. Imada, Phys. Rev. Lett. **91** 167203 (2003); New J. Phys. **6**, 154 (2004).
 [16] V. Anisimov *et al.*, J. Phys: Condens. Matter **9**, 7359 (1997); A. I. Lichtenstein and M. I. Katsnelson, Phys. Rev. B **57** 6884 (1998).
 [17] O. K. Andersen and T. Saha-Dasgupta, Phys. Rev B **62**, R16219 (2000); Bull. Mater. Sci. **26**, 19 (2003); Ref. [10].
 [18] F. Lechermann *et al.*, Phys. Rev. B **74**, 125120 (2006).
 [19] R. Fresard and G. Kotliar, Phys. Rev. B **56**, 12909 (1997).
 [20] A. Georges, G. Kotliar, W. Kraut, M. J. Rozenberg, Rev. Mod. Phys. **68**, 13 (1996).
 [21] J. E. Hirsch and R. M. Fye, Phys. Rev. Lett. **56**, 2521 (1986).
 [22] J. E. Gubernatis, M. Jarrell, R. N. Silver and D. S. Sivia, Phys. Rev. B **44**, 6011 (1991).
 [23] S. Miyasaka, Y. Okimoto, M. Iwama and Y. Tokura, Phys. Rev. B **68**, 100406(R) (2003).
 [24] See Eq.s (19)-(20), (23)-(26), and Fig. 18 of Ref. 10.
 [25] Compare orbitals in Fig. 2 with Fig. 14 of Ref. 10.
 [26] To prove this we performed LDA calculations using the titanates crystal structure and replacing Ti with V.
 [27] T. Arima, Y. Tokura and J. B. Torrance, Phys. Rev. B **48**, 17006 (1993); Y. Okimoto *et al.*, *ibid.* **51**, 9581 (1995); S. Miyasaka, Y. Okimoto and Y. Tokura, J. Phys. Soc. Jpn. **71**, 2086 (2002); A. A. Tsvetkov *et al.*, Phys. Rev. B **69**, 075110 (2004).
 [28] H. F. Pen *et al.*, Phys. Rev. B **59**, 7422 (1999); K. Maiti and D. D. Sarma, *ibid.* **61**, 2525 (2000).
 [29] O. Gunnarsson, E. Koch and R. M. Martin, Phys. Rev. B **54**, R11026 (1996); E. Koch, O. Gunnarsson, R. M. Martin, *ibid.* **60**, 15714 (1999).
 [30] J. E. Han, M. Jarrell and D. L. Cox, Phys. Rev. B **58**, R4199 (1998).
 [31] In Ref. [6] occupations are not for Wannier functions

- [1] Y. Ren *et al.*, Nature (London) **396**, 441 (1998); Y. Ren *et al.*, Phys. Rev. B **67**, 014107 (2003).
 [2] C. Ulrich *et al.*, Phys. Rev. Lett. **91**, 257202 (2003).
 [3] J.-Q. Yan, J.-S. Zhou and J. B. Goodenough, Phys. Rev. Lett. **93**, 235901 (2004).
 [4] H. Sawada *et al.*, Phys. Rev. B **53**, 12742 (1996); H. Sawada and K. Terakura, *ibid.* **58**, 6831 (1998); T. Mizokawa, D.I. Khomskii and G.A. Sawatzky, *ibid.* **60**, 7309 (1999).
 [5] M. Noguchi *et al.*, Phys. Rev. B **62**, R9271 (2000); M. Takahashi and J.I. Igarashi, *ibid.* **65**, 205114 (2002).
 [6] Z. Fang and N. Nagaosa, Phys. Rev. Lett. **93**, 176404 (2004). With their parameters ($U_{\text{eff}}=3$ eV, $J/U \sim 0.2$),

$(n_{t_{2g}} < 2)$, so a full comparison is not possible.